Measurement of the Q^2-dependence of the deuteron spin structure function g_1 and its moments at low Q^2 with CLAS

K.P. Adhikari[1,2,4], A. Deur[2,3,*] G.E. Dodge[1], L. El Fassi[1,4], H. Kang[5], S.E. Kuhn[1], M. Ripani[6], K. Slifer[3,7], X. Zheng[3], S. Adhikari[17], Z. Akbar[18], M.J. Amaryan[1], H. Avakian[2], J. Ball[12], I. Balossino[21], L. Barion[21], M. Battaglieri[6], I. Bedlinskiy[26], A.S. Biselli[15], P. Bosted[4]1, W.J. Briscoe[19], J. Brock[2], S. Bültmann[1], V.D. Burkert[2], Frank Thanh Cao[14], C. Carlin[2], D.S. Carman[2], A. Celentano[6], G. Charles[1], J.-P. Chen[2], T. Chetry[30], S. Choi[5], G. Ciullo[21], L. Clark[39], P.L. Cole[20,2], M. Contalbrigo[21], V. Crede[18], A. D'Angelo[23,33], N. Dashyan[42], R. De Vita[6], E. De Sanctis[22], M. Defurne[12], C. Djalali[35], V. Drozdov[6,34], R. Dupre[25], H. Egiyan[2,7], A. El Alaoui[37], L. Elouadrhiri[2], P. Eugenio[18], G. Fedotov[30,34], A. Filippi[24], Y. Ghandilyan[42], G.P. Gilfoyle[32], E. Golovatch[34], R.W. Gothe[35], K.A. Griffioen[41], M. Guidal[25], N. Guler[1], L. Guo[17,2], K. Hafidi[8], H. Hakobyan[37,42], C. Hanretty[2], N. Harrison[2], M. Hattawy[8], D. Heddle[13,2], K. Hicks[30], M. Holtrop[7], C.E. Hyde[1], Y. Ilieva[35,19], D.G. Ireland[39], E.L. Isupov[34], D. Jenkins[40], H.S. Jo[25], Sereres Johnston[8], K. Joo[14], S. Joosten[36], M.L. Kabir[4], C.D. Keith[2], D. Keller[3], G. Khachatryan[42], M. Khachatryan[1], M. Khandaker[29,20], A. Klein[1], F.J. Klein[11], P. Konczykowski[12], K. Kovacs[3], V. Kubarovsky[2,31], L. Lanza[23], P. Lenisa[21], K. Livingston[38], E. Long[7], I .J .D. MacGregor[38], N. Markov[14], M. Mayer[1], B. McKinnon[38], D.G. Meekins[2], C.A. Meyer[10], T. Mineeva[37], M. Mirazita[22], V. Mokeev[2,34], A Movsisyan[21], C. Munoz Camacho[25], P. Nadel-Turonski[2,19], G. Niculescu[27,30], M. Osipenko[6], A.I. Ostrovidov[18], M. Paolone[36], D. Payette[1], R. Paremuzyan[7], K. Park[2,28], E. Pasyuk[2,9], W. Phelps[17], S.K. Phillips[7], J. Pierce[3], O. Pogorelko[26], J. Poudel[1], Y. Prok[1,3], D. Protopopescu[38], B.A. Raue[17,2], A. Rizzo[23,33], G. Rosner[38], P. Rossi[1,22], F. Sabatié[12], C. Salgado[29], R.A. Schumacher[10], Y.G. Sharabian[2], T. Shigeyuki[3], A. Simonyan[25], Iu. Skorodumina[35,34], G.D. Smith[38], N. Sparveris[36], S. Stepanyan[2], I.I. Strakovsky[19], S. Strauch[35], V. Sulkosky[42], J.A. Tan[28], M. Ungaro[2,31], E. Voutier[25], X. Wei[2], L. Weinstein[1], J. Zhang[3,1], Z.W. Zhao[1,35]

[1] *Old Dominion University, Norfolk, Virginia 23529*
[2] *Thomas Jefferson National Accelerator Facility, Newport News, Virginia 23606*
[3] *University of Virginia, Charlottesville, Virginia 22901*
[4] *Mississippi State University, Mississippi State, Mississippi, MS 39762-5167*
[5] *Seoul National University, Seoul, Korea*
[6] *INFN, Sezione di Genova, 16146 Genova, Italy*
[7] *University of New Hampshire, Durham, New Hampshire 03824-3568*
[8] *Argonne National Laboratory, Argonne, Illinois 60439*
[9] *Arizona State University, Tempe, Arizona 85287-1504*
[10] *Carnegie Mellon University, Pittsburgh, Pennsylvania 15213*
[11] *Catholic University of America, Washington, D.C. 20064*
[12] *IRFU, CEA, Universit'e Paris-Saclay, F-91191 Gif-sur-Yvette, France*
[13] *Christopher Newport University, Newport News, Virginia 23606*
[14] *University of Connecticut, Storrs, Connecticut 06269*
[15] *Fairfield University, Fairfield CT 06824*
[16] *Universita' di Ferrara , 44121 Ferrara, Italy*
[17] *Florida International University, Miami, Florida 33199*
[18] *Florida State University, Tallahassee, Florida 32306*
[19] *The George Washington University, Washington, DC 20052*
[20] *Idaho State University, Pocatello, Idaho 83209*
[21] *INFN, Sezione di Ferrara, 44100 Ferrara, Italy*
[22] *IINFN, Laboratori Nazionali di Frascati, 00044 Frascati, Italy*
[23] *INFN, Sezione di Roma Tor Vergata, 00133 Rome, Italy*
[24] *INFN, Sezione di Torino, 10125 Torino, Italy*
[25] *Institut de Physique Nucléaire, CNRS/IN2P3 and Université Paris Sud, Orsay, France*
[26] *Institute of Theoretical and Experimental Physics, Moscow, 117259, Russia*
[27] *James Madison University, Harrisonburg, Virginia 22807*
[28] *Kyungpook National University, Daegu 41566, Republic of Korea*
[29] *Norfolk State University, Norfolk, Virginia 23504*
[30] *Ohio University, Athens, Ohio 45701*
[31] *Rensselaer Polytechnic Institute, Troy, New York 12180-3590*
[32] *University of Richmond, Richmond, Virginia 23173*
[33] *Universita' di Roma Tor Vergata, 00133 Rome Italy*
[34] *Skobeltsyn Institute of Nuclear Physics, Lomonosov Moscow State University, 119234 Moscow, Russia*
[35] *University of South Carolina, Columbia, South Carolina 29208*
[36] *Temple University, Philadelphia, PA 19122*
[37] *Universidad Técnica Federico Santa María, Casilla 110-V Valparaíso, Chile*

[38] *Edinburgh University, Edinburgh EH9 3JZ, United Kingdom*
[39] *University of Glasgow, Glasgow G12 8QQ, United Kingdom*
[40] *Virginia Tech, Blacksburg, Virginia 24061-0435*
[41] *College of William and Mary, Williamsburg, Virginia 23187-8795 and*
[42] *Yerevan Physics Institute, 375036 Yerevan, Armenia*

(Dated: October 27, 2017)

We measured the g_1 spin structure function of the deuteron at low Q^2, where QCD can be approximated with chiral perturbation theory (χPT). The data cover the resonance region, up to an invariant mass of $W \approx 1.9$ GeV. The generalized GDH sum, the moment Γ_1^d and the spin polarizability γ_0^d are precisely determined down to a minimum Q^2 of 0.02 GeV^2 for the first time, about 2.5 times lower than that of previous data. We compare them to several χPT calculations and models. These results are the first in a program of benchmark measurements of polarization observables in the χPT domain.

PACS numbers: 13.60.Hb, 11.55.Hx,25.30.Rw, 12.38.Qk

INTRODUCTION

For the last three decades, the spin structure of the nucleon has been actively investigated experimentally and theoretically [1, 2]. The reason is that the nucleon structure is dominated by the strong interaction – the least known fundamental force in the experimentally reachable domain – and that including spin degrees of freedom offers a more complete description of nucleon structure. The first studies of the nucleon spin structure involved inclusive reactions, which are still the origin of most of our current knowledge, and are the object of the experiment reported here. Generalized parton distributions and transverse momentum dependent parton distributions are now becoming available and are necessary to complete the picture of the nucleon spin. Apart from the technological feats of developing the polarized targets and beams necessary for such studies, the first challenge encountered in this endeavor was the "spin crisis": the realization that the quark spins contribute much less than expected to the proton spin [3]. It is now understood that this unexpected feature points to previously neglected contributions, like gluon spin and orbital angular momentum. Thus, a prominent focus of nucleon spin study is to measure each individual contribution to the nucleon's spin. At the same time, it was realized that sum rules could also be used to address other challenging questions about Quantum chromodynamics (QCD, the gauge theory describing the strong interaction) [4]: quark confinement and how the low energy effective degrees of freedom of QCD (baryons and mesons) are related to its fundamental ones (quarks and gluons).

This article reports on a measurement pertaining to this latter topic: it provides the first precise measurement of the Q^2-evolution of the generalized Gerasimov-Drell-Hearn (GDH) integral [5, 6] and of the spin polarizability γ_0 [7] on the deuteron at very low four-momentum transfer Q^2. Such a measurement allows us to test chiral perturbation theory (χPT) – a low Q^2 approximation of QCD – which has been challenged by earlier measurements of the GDH integral and of spin polarizabilities [8–14]. These measurements were dedicated, however, to study the transition between the perturbative and non-perturbative domains of QCD and were performed at higher Q^2. Only their lowest Q^2 points (0.05 GeV^2 for H and D and 0.1 GeV^2 for ^{3}He) reached the χPT domain and had limited precision. The experimental results reported here are from the Jefferson Lab (JLab) CLAS EG4 experiment, specifically dedicated to measure the proton, deuteron and neutron polarized inclusive cross-section at significantly lower Q^2 than previously measured. A complementary program exists in JLab's Hall A, dedicated to the neutron (from ^{3}He) [15] and to the transversely polarized proton [16].

An additional goal of EG4 was to assess the reliability of extracting neutron structure information from measurements on nuclear target. The deuteron and ^{3}He complement each other for neutron information: nuclear binding effects in the deuteron are smaller than for ^{3}He, but to obtain the neutron information a large proton contribution needs to be subtracted. The proton contributions in ^{3}He are small, making polarized ^{3}He nearly a polarized neutron target. However, the tightly bound nucleons in ^{3}He have larger nuclear binding effects and non-nucleonic degrees of freedom may play a larger role.

THE GDH AND γ_0 SUM RULES

Sum rules relate an integral over a dynamical quantity to a global property of the object under study. They offer stringent tests of the theories from which they stem. The Bjorken [17] and the GDH [5, 6] sum rules are important examples. The latter was originally derived for photoproduction, $Q^2 = 0$, and links the helicity-dependent photoproduction cross-sections σ_A and σ_P to the anomalous

*Contact author. Email: deurpam@jlab.org

magnetic moment κ of the target:

$$\int_{\nu_0}^{\infty} \frac{\sigma_A(\nu) - \sigma_P(\nu)}{\nu} d\nu = -\frac{4\pi^2 S\alpha\kappa^2}{M^2}, \qquad (1)$$

where M is the mass of the object, S its spin, α the QED coupling, ν the photon energy and ν_0 the photoproduction threshold. The A and P correspond to the cases where the photon spin is anti-parallel and parallel to the object spin, respectively. For the deuteron, $S = 1$ and $-4\pi^2 S\alpha\kappa^2/M^2 = -0.6481(0)$ μb. The GDH sum rule originates from a dispersion relation and a low energy theorem that are quite general and do not depend on QCD. The only assumption involves the convergence necessary to validate the dispersion relation. As such, the sum rule is regarded as a solid general prediction, and experiments at MAMI, ELSA and LEGS [18] have verified the validity of the sum rule within about 7% precision for the proton. Verifying the sum rule on the neutron is more difficult since no free-neutron targets exist. Deuteron data taken at MAMI, ELSA and LEGS cover up to $\nu = 1.8$ GeV [18] but have not yet tested the sum rule due to the delicate cancellation of the deuteron photo-disintegration channel ($\approx 400\mu$b) with the other inelastic channels ($\approx 401\mu$b) [19].

In the midst of the "spin crisis", it was realized that the GDH integral could be extended to electroproduction and that it could be used to study the transition between the perturbative and non-perturbative domains of QCD [4]. A decade later, the sum rule itself was generalized [20]:

$$\begin{aligned} &\frac{M^2}{4\pi^2\alpha}\int_{\nu_0}^{\infty} \frac{\Gamma_v(\nu,Q^2)}{\nu}\frac{\sigma_A(\nu,Q^2) - \sigma_P(\nu,Q^2)}{\nu} d\nu \\ &= \frac{2M^2}{Q^2}\int_0^{x_0} \Big[g_1(x,Q^2) - \frac{4M^2}{Q^2}x^2 g_2(x,Q^2)\Big] dx \\ &= I_{TT}(Q^2), \end{aligned} \qquad (2)$$

where I_{TT} is the spin-flip double-virtual Compton scattering (VVCS) amplitude in the $\nu \to 0$ limit, Γ_v is the virtual photon flux, g_1 and g_2 are the two inclusive spin structure functions, x is the Bjorken scaling variable defined as $x = Q^2/2M\nu$, and x_0 is the electroproduction threshold. A slightly different version of the generalized GDH sum rule is [21]:

$$\frac{2M^2}{Q^2}\int_0^{x_0} g_1(x,Q^2)dx = I_1(Q^2), \qquad (3)$$

where I_1 is the $\nu \to 0$ limit of the first covariant polarized VVCS amplitude. An advantage of this generalization is that it establishes a direct connection with the Bjorken sum rule [17], the isovector version of I_1 with $I_1^{p-n}Q^2M^2 = g_a/3$ for $Q^2 \to \infty$ (g_a is the nucleon axial charge). Both generalized sum rules in Eqs. (2) and (3) recover the original GDH sum rule at $Q^2 = 0$.

What makes the generalized GDH sum rule valuable is that it offers a fundamental relation for any Q^2. In the low and high Q^2 limits where I_1 or I_{TT} can be related to global properties of the target, this sum rule can be used to test our understanding of the nucleon spin structure. At intermediate Q^2 it tests the non-perturbative QCD calculations of I_1 or I_{TT}: while lattice gauge theory results for GDH are still unavailable, previous data have been used to test the AdS/QCD approach [22], phenomenological models of the nucleon structure [23] and χPT calculations [24–26] at lower Q^2.

An ancillary result of the present low-Q^2 data is their extrapolation to $Q^2 = 0$ in order to check the sum rule on $\approx$(proton+neutron) [19] and on the neutron. Although the extrapolation adds an uncertainty to this determination, the inclusive electron scattering used in this work sums all reaction channels without the need to detect final state particles, thereby allowing measurement of the whole sum rule integrand, unlike photoproduction that requires detecting each final state, with more associated systematic uncertainties .

The GDH and Bjorken sum rules involve the first moment of the spin structure functions. Other sum rules exist that employ higher moments such as the spin polarizability γ_0 sum rule [21]:

$$\begin{aligned} \gamma_0(Q^2) \;&=\; \frac{1}{2\pi^2}\int_{\nu_0}^{\infty} \frac{\Gamma_v(\nu,Q^2)}{\nu}\frac{\sigma_A(\nu,Q^2) - \sigma_P(\nu,Q^2)}{\nu^3} d\nu \\ &= \frac{16\alpha M_t^2}{Q^6}\int_0^{x_0} x^2\Big[g_1(x,Q^2) - \frac{4M^2}{Q^2}x^2 g_2(x,Q^2)\Big] dx. \end{aligned} \qquad (4)$$

An advantage of the polarizability is that the kinematic weighting highly suppresses the low-x contribution to the sum rule, which typically must be estimated with model input since it is inaccessible by experiment. For this reason, γ_0 provides a robust test of χPT, although it has a high sensitivity to how data is extracted at the inelastic threshold. γ_0 has been measured at MAMI for $Q^2 = 0$ and at JLab on the proton, neutron and deuteron for $0.05 \le Q^2 \le 4$ GeV^2 [10–14].

The JLab data revealed unexpected discrepancies with χPT calculations for γ_0, its isovector and isoscalar components, and the generalized longitudinal-transverse spin polarizability δ_{LT}^n [10–13]. The data for γ_0, and I_1 typically agree only for the lowest Q^2 points investigated ($Q^2 \lesssim 0.07$ GeV^2) and generally only with one type of χPT calculations: for a given observable, the results of Ref. [24] would agree and the ones of Ref. [25] would not, while the opposite occurs for another observable. Furthermore, the experimental and theoretical uncertainties of the first generation of experiments and calculations limited the usefulness of these comparisons. Conversely, I_1^{p-n} was found to agree well with χPT [12]. No data on δ_{LT}^p exist although some are anticipated soon [16]. This state of affairs triggered a refinement of the χPT calculations [24–26] and a very low Q^2 experimental program to test them.

MEASUREMENTS

The EG4 experiment took place in 2006 at JLab using the CLAS spectrometer in Hall B [27]. The aim was to measure g_1^p and g_1^d over a x-range large enough to provide most of the generalized GDH integral, and over a Q^2-range covering the region were χPT should apply. The inclusive scattering of polarized electrons off longitudinally polarized protons or deuterons was the reaction of interest, but exclusive ancillary data were also recorded [28]. For the deuteron run, two incident electron beam energies were used, 1.3 GeV and 2.0 GeV. The CLAS spectrometer was equipped with a new Cherenkov Counter (CC) in one of its sectors to improve the forward angle detection. The target position was moved 1 m upstream of the nominal CLAS center to reach smaller scattering angles and the toroidal magnetic field of CLAS bent electrons outward, yielding a minimum scattering angle of about 6^o. This resulted in a coverage of $0.02 \leq Q^2 \leq 0.84$ GeV^2 and of invariant mass $W \leq 1.9$ GeV.

The polarized beam was produced by illuminating a strained GaAs cathode with a polarized diode laser. A Pockels cell flipped the beam helicity pseudo-randomly at 30 Hz and a half-wave plate was inserted periodically to provide an additional change of helicity sign to cancel possible false beam asymmetries. The beam polarization varied around 85±2% and was monitored with a Møller polarimeter [27]. The beam current ranged between 1 and 3 nA.

The polarized deuteron target consisted of $^{15}ND_3$ ammonia beads held in a 1K ^{4}He bath, and placed in a 5 T field [29]. The target was polarized using dynamical nuclear polarization. The polarization was enhanced *via* irradiation with microwaves. The target polarization was monitored by a nuclear magnetic resonance (NMR) system and ranged between 30% and 45%. The polarization orientation was always along the beam direction. The target diameter was 1.5 cm and its physical length was 1 cm. The NMR and Møller-derived polarizations were used for monitoring only, the product of the beam and target polarizations for the analysis being provided through the measured asymmetry of quasi-elastic scattering. To evenly spread beam heating and depolarization, the beam was rastered over the target with a spiral pattern with a 1.2 cm diameter repeated every 2 s.

The scattered electrons were detected by the CLAS spectrometer. Besides the new CC used for data acquisition triggering and electron identification, CLAS contained three multi-layer drift chambers that provided the momenta and charges of the scattered particles, time-of-flight counters and electromagnetic calorimeters (EC) for further particle identification. The trigger for the data acquisition system was provided by a coincidence between the new CC and the EC. Supplemental data were taken with an EC-only trigger for efficiency measurements. Further information on EG4 can be found in Refs. [28, 30].

ANALYSIS

The spin structure function g_1 was extracted in W and Q^2 bins from the measured difference in normalized yields between anti-parallel and parallel beam and target polarizations:

$$\frac{N^{\uparrow\Downarrow}(W,Q^2)}{Q_b^{\uparrow\Downarrow}} - \frac{N^{\uparrow\Uparrow} - (W,Q^2)}{Q_b^{\uparrow\Uparrow}} = \mathcal{L} P_b P_t \Delta\sigma(W,Q^2) a(W,Q^2), \quad (5)$$

where "$\uparrow\Downarrow$ or "$\uparrow\Uparrow$" refers to beam spin and target polarization being anti-parallel or parallel, respectively. N is the number of counts and Q_b is the corresponding integrated beam charge. $\mathcal{L}$ is a constant corresponding to the density of polarized target nuclei per unit area, $P_b P_t$ is the product of the beam and target polarizations and $a(W,Q^2)$ is the detector acceptance, which also accounts for detector, trigger and cut efficiencies. The cross-section difference $\Delta\sigma$ is defined as:

$$\Delta\sigma \equiv \frac{d\sigma^{\uparrow\Downarrow}}{\Delta\Omega dE'} - \frac{d\sigma^{\uparrow\Uparrow}}{\Delta\Omega dE'}, \quad (6)$$

where E' is the energy of the scattered electron. In the Born approximation,

$$\Delta\sigma = \frac{4\alpha^2}{MQ^2}\frac{E'}{E}\left[\frac{g_1}{\nu}(E + E'\cos\theta) - Q^2\frac{g_2}{\nu^2}\right], \quad (7)$$

with θ the polar scattering angle. Only polarized material contributes to $\Delta\sigma$, which is advantageous due to the dilution factor of the polarized targets used by EG4.

The product of the polarized luminosity, beam and target polarization, $P_b P_t$, and the overall electron detection efficiency was determined by comparing the measured yield difference in the quasi-elastic region, $0.9 < W < 1$ GeV, with the calculated values. An event generator based on RCSLACPOL [31], with up-to-date models of structure functions and asymmetries for inelastic scattering from deuterium [14], was used to generate events according to the fully radiated cross section in Eq. (7). The events were followed through a full simulation of the CLAS spectrometer based on a Geant-3 simulation package. Thus, the simulated events were analyzed in the same way as the measured data, thereby accounting for the bin-to-bin variation of acceptance and efficiency (Eq. (5)). A comparison between the simulated and the measured data in a given Q^2 bin is shown in Fig. 1. Any deviation between the simulation and the experimental results can be due to two possible sources: 1) A genuine difference between the g_1 models and the

true value within that bin; 2) systematic deviations of all other ingredients entering the simulation from their correct values: this includes backgrounds and detector efficiencies and distortions, as well as models for other structure functions (F_2, R) and asymmetries (A_2) and radiative effects. To extract $g_1(W,Q^2)$ from our measured data, we determined the amount δg_1 by which the model for g_1 had to be varied in a given bin to fully account for the difference between measured and simulated yield difference:

$$\begin{aligned}\delta g_1 &= g_1^{data}(W,Q^2) - g_1^{Model}(W,Q^2) \\ &= \frac{\Delta n^{data}(W,Q^2) - \Delta n^{standard}(W,Q^2)}{(\partial \Delta n/\partial g1)_{simulated}}, \end{aligned} \quad (8)$$

where n is the number of counts and the values Δn^{data} and $\Delta n^{standard}$ come from the polarized yield differences Δn in the data and the standard simulation, respectively. The systematic uncertainty on g_1 due to each of the sources in 2) above was determined by varying one of the ingredients within their reasonable uncertainties and extracting the corresponding impact on g_1 accordingly. It is important to understand that although a model is used for obtaining g_1, there is little model-dependence in the results reported here.

Cuts were used for particle identification, to reject events not originating from the target, to select detector areas of high acceptance and high detector efficiency, where the detector simulation reproduces well the data [30]. Corrections were applied for contaminations from π^- and from secondary electrons produced from $\gamma \to e^-e^+$ (with the γ produced mostly from π^0 decay). The π^- contamination was typically around 1% or less and pair-symmetric electrons amounted to a correction of less than 3% in nearly all cases. Quality checks were performed, including detector and yield stability with time. Vertex corrections to account for the beam raster, any target-detector misalignments and toroidal field mapping inaccuracies, were determined and applied. Electron energy loss by ionization in the target or detector material were corrected for, as well as bremsstrahlung and other radiative corrections.

Systematic uncertainties are typically of order 10% of the extracted values for $g_1(x,Q^2)$ and nearly always smaller than statistical uncertainties. They are dominated by the overall normalization uncertainty (about 7-10%, depending on kinematic bin), model uncertainties for unmeasured quantities (up to 10% in a few kinematic bins, but normally smaller), and radiative correction and kinematic uncertainties (up to 5% near threshold but much smaller elsewhere). The model uncertainties were estimated by modifying the parameters controlling $g_1(x,Q^2)$ and $g_2(x,Q^2)$. The calculation and comparison of these contributions is detailed in Ref. [30].

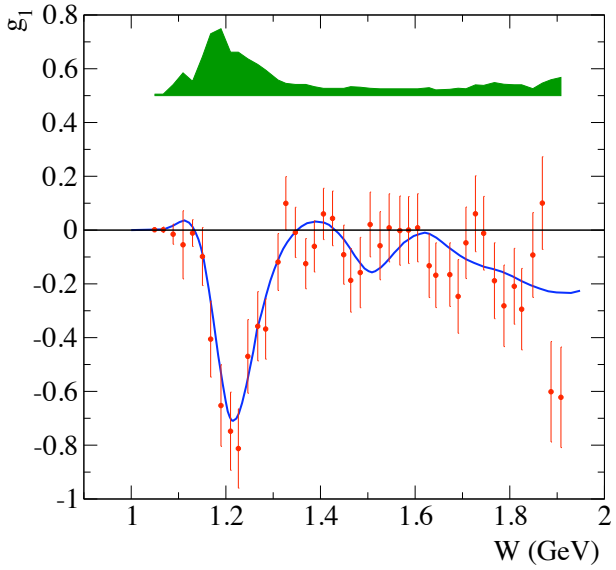

FIG. 1: Example of extracted $g_1^d(W)$ vs. invariant mass W (circles), together with the nominal value of the parameterization used for its extraction (line). The large negative peak corresponds to the $\Delta(1232)$ $3/2^+$ resonance. The error bars give the statistical uncertainty and the band is the total systematic uncertainty. The data are for $\langle Q^2 \rangle = 0.1$ GeV^2.

RESULTS ON THE GDH AND γ_0 INTEGRALS

The integrals in Eqs. (3)-(4) are formed by integrating the data over the $x_{min} < x < x_0$ range, where x_{min} is the lowest x reached by the experiment for a given Q^2 bin. For the lowest Q^2 bin, 0.020 GeV^2, $x_{min} = 0.0073$, and for the largest Q^2 bin considered for integration, 0.592 GeV^2, $x_{min} = 0.280$. The data are supplemented by the model to cover the integration range $0.001 < x < x_{min}$. The correction for the quasi-elastic contamination below x_0 is done using the model [30].

The integral $\Gamma_1^d(Q^2) \equiv \frac{Q^2}{2M^2} I_1(Q^2)$ is shown in Fig. 2. The original GDH sum rule provides the derivative of Γ_1 at $Q^2 = 0$. The low-x correction is small. The full integral (blue squares) agrees with the previous CLAS EG1b experiment [14], but the minimum Q^2 is 2.5 times lower. The statistical uncertainty of EG4 is improved over EG1b by about a factor of 4 at the lowest Q^2 points and thus allows for a more stringent test of χPT. The Lensky *et al.* χPT calculation [26], which supersedes the earlier calculations in Ref. [25], agrees with the data. The most recent Bernard *et al.* χPT calculations [24] agree with the few lowest Q^2 points. The Pasechnik *et al.* and Burkert-Ioffe models [23] describe the data well.

The data can also be integrated to form the related moment $\bar{I}_{TT}^d(Q^2)$ (Eq. (2)), shown in Fig. 3. The bar over I_{TT}^d indicates that the integral excludes the electrodisintegration contribution. We do not include the channels below the pion production threshold because the CLAS resolution is not high enough for an accurate inte-

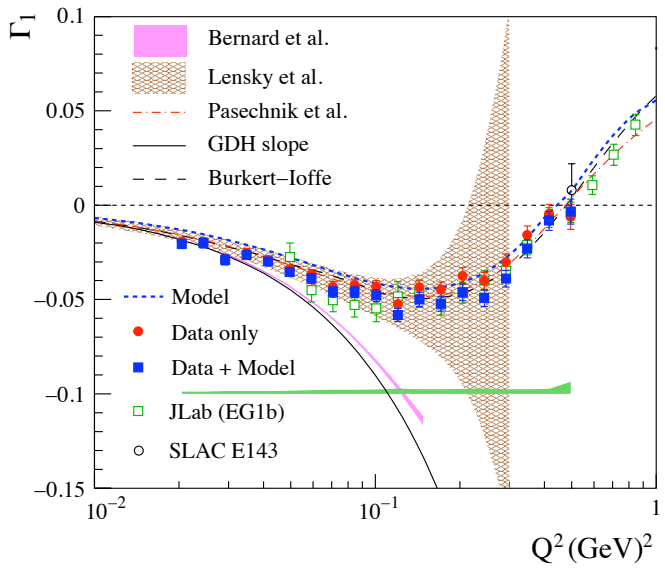

FIG. 2: The first moment $\Gamma_1^d(Q^2)$.The circles are the EG4 data integrated over the covered kinematics. The fully integrated Γ_1^d, using a model to supplement data, is shown by the squares. The error bars are statistical. The systematic uncertainty is given by the horizontal band. The open symbols show data from the CLAS EG1b [14] and SLAC E143 [31] experiments. The other bands and lines show various models and χPT calculations as described in the text.

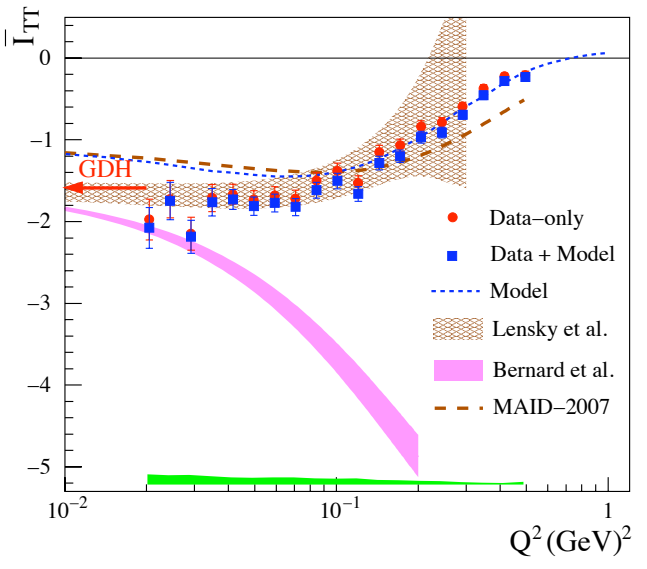

FIG. 3: The generalized GDH integral $\bar{I}_{TT}(Q^2)$. For legends and theoretical calculations, see Fig. 2. The arrow indicates the expectation from the original GDH sum rule.

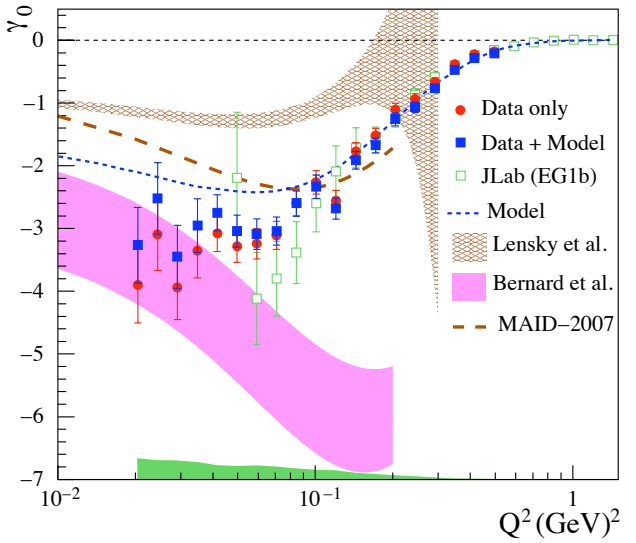

FIG. 4: The generalized spin polarizability $\gamma_0(Q^2)$. See Fig. 2 for legends and theoretical calculations.

gration. The Lensky *et al.* χPT calculation [26] agrees with the data in the entire calculated range. As for Γ_1^d, the Bernard *et al.* χPT calculation [24] agrees with the few lowest Q^2 points. In addition to testing χPT, the EG4 data can be extrapolated to $Q^2 = 0$ and compared with the original sum rule expectation that $I_{TT}(0) = -\kappa^2/4$. Accounting for the deuteron D-state and ignoring the deuteron breakup and the coherent channel, the GDH sum rule predicts $\bar{I}_{TT}^d = (1-3\omega_D/2)(I_{TT}^p + I_{TT}^n) = -1.574 \pm 0.026$, with $\omega_D = 0.056 \pm 0.01$ [32]. We extrapolated to $Q^2 = 0$ the data below $Q^2 = 0.06$ GeV^2, which average at $\langle Q^2 \rangle = 0.045$ GeV^2. To this end, we used the (small) Q^2-dependence of the Lensky *et al.* calculation [26] since it agrees very well with the data. We find $\bar{I}_{TT}^{d\ exp}(0) = -1.724 \pm 0.027(stat) \pm 0.050(syst)$. This is 10% away from the sum rule prediction of -1.574 ± 0.026, which represents $\approx 1.5\sigma$. This can be compared with the MAMI and ELSA measurement with real photons: $\bar{I}_{TT}^{d\ exp}(0) = -1.986 \pm 0.008(stat) \pm 0.010(syst)$ integrated over $0.2 < \nu < 1.8$ GeV (the systematic uncertainties here do not include any low and large ν contributions) [18]. Using the proton GDH sum rule world data [18], we deduce the neutron GDH integral $I_{TT}^{n\ exp}(0) = -0.955 \pm 0.040(stat) \pm 0.113(syst)$, which agrees within uncertainties with the sum rule expectation $I_{TT}^{n\ theo}(0) = -0.803$.

Finally, the generalized spin polarizability $\gamma_0(Q^2)$ can be formed from Eq. (4) and is shown in Fig. 4. The Pasechnik *et al.* and Burkert-Ioffe models are not available for γ_0. The MAID prediction, a multipole analysis of photo- and electroproduced resonance data up to $W = 2$ GeV [33], is relevant since the low-x contribution, not included in MAID, is largely suppressed. The χPT calculations differ markedly. The full γ_0 from EG4 (blue squares) agrees with the Bernard *et al.* χPT calculation [24] and disagree with the Lensky *et al.* χPT calculation [26] and with the MAID model below 0.07 GeV^2.

SUMMARY AND CONCLUSION

We report the first precise measurement of the Q^2-evolution of the generalized GDH integral and of the spin polarizability γ_0 on the deuteron in the $0.02 < Q^2 < 0.59$ GeV^2 domain. The data reach a minimal Q^2 2.5 times lower than that of previously available data, with much improved precision. The data in general agree with χPT predictions, although the degree of agreement of the different χPT methods varies with the observable: the Bernard *et al.* χPT calculations are more successful with γ_0, while the Lensky *et al.* ones are more successful with the GDH integral. The phenomenological models of Pasechnik *et al.* and Burkert-Ioffe agree well with the GDH data. The MAID model disagrees with the γ_0 data for $Q^2 \leq 0.07$ GeV^2.

The data can be extrapolated to $Q^2 = 0$ to compare with the GDH sum rule expectation summed over the proton and neutron. Because the deuteron integral does not include the photo-disintegration contribution, the data test the GDH sum rule on the proton+neutron. The extrapolated data are 10% away from the expectation, which represents $\approx 1.5\sigma$. For the neutron, they are 20% away from the expectation, which represents $\approx 1.0\sigma$. Hence, the sum rules seem to be satisfied within this precision.

The program of providing benchmark polarization observables for χPT will be completed when the proton EG4 data become available, as well as the longitudinally and the transversally polarized data on the neutron (^{3}He) [15] and proton [16] from JLab's Hall A.

This work was supported by: the U.S. Department of Energy (DOE), the U.S. National Science Foundation, the U.S. Jeffress Memorial Trust; the Physics and Astronomy Department and the Office of Research and Economic Development at Mississippi State University, the United Kingdoms Science and Technology Facilities Council (STFC) under grant numbers, the Italian Istituto Nazionale di Fisica Nucleare; the French Institut National de Physique Nucléaire et de Physique des Particules, the French Centre National de la Recherche Scientifique; and the National Research Foundation of Korea. This material is based upon work supported by the U.S. Department of Energy, Office of Science, Office of Nuclear Physics under contract DE-AC05-06OR23177.

[1] S. E. Kuhn, J.-P. Chen and E. Leader, Prog. Part. Nucl. Phys. **63**, 1 (2009); J. P. Chen, Int. J. Mod. Phys. E **19**, 1893 (2010).

[2] For a recent review, see C. A. Aidala, S. D. Bass, D. Hasch and G. K. Mallot, Rev. Mod. Phys. **85**, 655 (2013).

[3] J. Ashman *et al.* [European Muon Collaboration], Phys. Lett. B **206**, 364 (1988).

[4] M. Anselmino, B. L. Ioffe and E. Leader, Sov. J. Nucl. Phys. **49**, 136 (1989) [Yad. Fiz. **49**, 214 (1989)].

[5] S. B. Gerasimov, Sov. J. Nucl. Phys. **2**, 430 (1966) [Yad. Fiz. **2**, 598 (1965)]; S. D. Drell and A. C. Hearn, Phys. Rev. Lett. **16**, 908 (1966); M. Hosoda and K. Yamamoto Prog. Theor. Phys. 36 (2), 425 (1966).

[6] For a review of the sum rule and its verification, see: K. Helbing, Prog. Part. Nucl. Phys. **57**, 405 (2006).

[7] P. A. M. Guichon, G. Q. Liu and A. W. Thomas, Nucl. Phys. A **591**, 606 (1995).

[8] M. Amarian *et al.*, Phys. Rev. Lett. **89**, 242301 (2002); Phys. Rev. Lett. **92**, 022301 (2004); A. Deur *et al.*, Phys. Rev. Lett. **93**, 212001 (2004).

[9] K. Slifer *et al.* Phys. Rev. Lett. **101**, 022303 (2008).

[10] J. Yun *et al.* [CLAS Collaboration], Phys. Rev. C **67**, 055204 (2003); R. Fatemi *et al.* [CLAS Collaboration], Phys. Rev. Lett. **91**, 222002 (2003); K. V. Dharmawardane *et al.* [CLAS Collaboration], Phys. Lett. B **641**, 11 (2006); Y. Prok *et al.* [CLAS Collaboration], Phys. Lett. B **672**, 12 (2009).

[11] M. Amarian *et al.* [E94010 Collaboration], Phys. Rev. Lett. **93**, 152301 (2004).

[12] A. Deur *et al.*, Phys. Rev. D **78**, 032001 (2008).

[13] R. G. Fersch *et al.* (CLAS Collaboration), Accepted in Phys. Rev. C (2017) [arXiv:1706.10289].

[14] N. Guler *et al.* [CLAS Collaboration], Phys. Rev. C **92**, no. 5, 055201 (2015).

[15] V. Sulkosky *et al.* In preparation.

[16] JLab E08-027, K. Slifer, A. Camsonne, J.-P. Chen and D. Crabb spokespersons. http://hallaweb.jlab.org/experiment/g2p/docs/PAC33/dlt.pdf

[17] J. D. Bjorken, Phys. Rev. **148**, 1467 (1966); Phys. Rev. D **1**, 1376 (1970).

[18] J. Ahrens *et al.* [GDH and A2 Collaborations], Phys. Rev. Lett. **87**, 022003 (2001), Phys. Rev. Lett. **97**, 202303 (2006); H. Dutz *et al.* [GDH Collaboration], Phys. Rev. Lett. **91**, 192001 (2003); Phys. Rev. Lett. **93**, 032003 (2004); Phys. Rev. Lett. **94**, 162001 (2005); S. Hoblit *et al.* [LSC Collaboration], Phys. Rev. Lett. **102**, 172002 (2009).

[19] In this paper, we exclude most of the deuteron break-up channel by requiring $W = \sqrt{M^2 + 2M\nu - Q^2} > 1.15$ GeV. In that case, the integrals are close to the incoherent sums of the corresponding integrals for the proton and the neutron, modified by the deuteron D-state correction factor.

[20] X. D. Ji and J. Osborne, J. Phys. G **27**, 127 (2001).

[21] D. Drechsel, B. Pasquini and M. Vanderhaeghen, Phys. Rept. **378**, 99 (2003).

[22] S. J. Brodsky, G. F. de Teramond and A. Deur, Phys. Rev. D **81**, 096010 (2010).

[23] V. Burkert and Z. j. Li, Phys. Rev. D **47**, 46 (1993); V. D. Burkert and B. L. Ioffe, Phys. Lett. B **296**, 223 (1992); J. Exp. Theor. Phys. **78**, 619 (1994) [Zh. Eksp. Teor. Fiz. **105**, 1153 (1994)]; R. S. Pasechnik, J. Soffer and O. V. Teryaev, Phys. Rev. D **82**, 076007 (2010).

[24] V. Bernard, N. Kaiser and U. G. Meissner, Phys. Rev. D **48**, 3062 (1993); V. Bernard, T. R. Hemmert and U. G. Meissner, Phys. Lett. B **545**, 105 (2002); V. Bernard, T. R. Hemmert and U. G. Meissner, Phys. Rev. D **67**, 076008 (2003); V. Bernard, E. Epelbaum, H. Krebs and U. G. Meissner, Phys. Rev. D **87**, no. 5, 054032 (2013).

[25] X. D. Ji, C. W. Kao and J. Osborne, Phys. Lett. B **472**, 1 (2000); Phys. Rev. D **61**, 074003 (2000); C. W. Kao, T. Spitzenberg and M. Vanderhaeghen, Phys. Rev. D **67**, 016001 (2003).

[26] V. Lensky, J. M. Alarcon and V. Pascalutsa, Phys. Rev. C **90**, no. 5, 055202 (2014).

[27] B. A. Mecking *et al.*, Nucl. Instrum. Meth. A **503**, 513 (2003).

[28] X. Zheng *et al.* [CLAS Collaboration], Phys. Rev. C **94**, no. 4, 045206 (2016).

[29] D. G. Crabb and D. B. Day, Nucl. Instrum. Meth. A **356**, 9 (1995); C. D. Keith *et al.*, Nucl. Instrum. Meth. A **501**, 327 (2003).

[30] K. Adhikari Ph.D. dissertation, 2013. www.jlab.org/Hall-B/general/thesis/Adhikari_thesis.pdf

[31] K. Abe *et al.* [E143 Collaboration], Phys. Rev. D **58**, 112003 (1998).

[32] M. Lacombe *et al.,* Phys. Rev. **C 21**, 861 (1980); R. Machleidt, K. Holinde, C. Elster, Phys. Rept. **149**, 1 (1987); M. J. Zuilhof, J. A. Tjon, Phys. Rev. **C 22**, 2369 (1980); K. Kotthoff, R. Machleidt, D. Schutte, Nucl. Phys. **A 264**, 484 (1976); B. Desplanques, Phys. Lett. **B 203**, 200 (1988).

[33] D. Drechsel, S. Kamalov and L. Tiator. Nucl. Phys. **A 645**, 145 (1999).